Available online at www.sciencedirect.com
SCIENCE DIRECT®
Journal of Sound and Vibration 269 (2004) 135–164
JOURNAL OF SOUND AND VIBRATION
www.elsevier.com/locate/jsvi

A basic hybrid finite element formulation for mid-frequency analysis of beams connected at an arbitrary angle

X. Zhao, N. Vlahopoulos*

Department of Naval Architecture and Marine Engineering, University of Michigan, 2600 Draper Road, Ann Arbor, MI 48109-2145, USA

Received 9 July 2001; accepted 4 December 2002

Abstract

When beams are connected at an arbitrary angle and subjected to an external excitation, both longitudinal and bending waves are generated in the system. Since longitudinal wavelengths are considerably longer than bending wavelengths in the mid-frequency region, the number of bending wavelengths in the beams is considerably larger than the number of longitudinal wavelengths. In this paper, plannar beams connected at arbitrary angles are considered. The energy finite element analysis (EFEA) is employed for modelling the bending behavior of the beams and the conventional finite element analysis (FEA) is utilized for modelling the longitudinal vibration in the beams. Thus, a basic hybrid FEA formulation is presented for mid-frequency analysis of systems that contain two types of energy. The bending vibration is associated with the long members in the system and the longitudinal vibration is associated with the short members. The long members are considered to have high modal overlap and to contain several wavelengths within their dimension, and uncertainty effects are present. The short members contain a small number of wavelengths, and exhibit a low modal overlap. Due to the low modal overlap the resonant frequencies are spaced far apart in the frequency domain, therefore the short members exhibit resonant or non-resonant behavior depending on the frequency of the excitation.

In this work, the bending and the longitudinal vibration within the same beam member are treated as a long and as a short member, respectively. A hybrid joint formulation is developed between long and short members. Power reflection and transmission coefficients are derived for each joint. The distribution of the energy throughout the system demonstrates a strong dependency on the power transfer coefficients. Several

*Corresponding author. Tel.: +1-734-764-8341; fax: +1-734-936-8820.
E-mail address: nickvl@engin.umich.edu (N. Vlahopoulos).

0022-460X/03/$ - see front matter
doi:10.1016/S0022-460X(03)00038-5

systems are analyzed by the hybrid FEA and by analytical solutions, and good correlation between them is observed.

1. Introduction

The frequency spectrum where simulation methods can be utilized for vibration analysis can be divided into three regions: low, mid, and high frequency. The low-frequency region is defined as the frequency range where all components contain a small number of wavelengths (short members). Due to the relative large size of the wavelengths with respect to the size of each component small uncertainties in the properties of the short members do not impact their distinctly resonant behavior. By taking into account the definition of the modal overlap as the resonance bandwidth divided by the average frequency spacing between resonance frequencies it is expected that short members will have low modal overlap values and exhibit resonant behavior. conventional finite element analysis (FEA) is a practical numerical approach for simulating low-frequency vibrations [1–3].

In the high-frequency region all the component members of a system are long with respect to a wavelength (long members). Due to the relative small size of the wavelengths with respect to the size of each component, small uncertainties in the properties of the long members lead to a behavior that can be considered as incoherent. In addition, long members are expected to exhibit considerably higher modal overlap than the short members, since resonant effects are not present. Statistical energy analysis (SEA) [4–8], and energy finite element analysis (EFEA) [9–15] can be used for vibro-acoustic simulations at high frequencies. Both methods provide meaningful results for the ensemble average response of each member and of the system [16].

The mid-frequency region is defined as the frequency range where some of the components of a system behave as long members while other members present characteristics of short members. In the mid-frequency range the FEA method requires a prohibiting large number of computations in order to capture the discrete in space and frequency vibration of the long members and in order to include uncertainty effects. The energy methods (SEA and EFEA) contain assumptions that are valid when all components of a system exhibit behavior that can be approximated as incoherent. Thus, the energy methods cannot capture the resonant effects which are present due to the short members of a system in the mid-frequencies. In the energy methods the amount of power transferred between members at a joint is defined in terms of coupling loss factors (in SEA) or power transfer coefficients (in EFEA). The process that computes the values of the coupling loss factors or the power transfer coefficients employs analytical solutions of semi-infinite members in order to define the power transfer characteristics of each joint [17]. The computations are meaningful when the members connected at the joint are long and their power transfer characteristics can be considered as equal to the power transfer characteristics of the semi-infinite members due to the high modal overlap of the members. The requirement for high modal overlap is necessary because the information produced by the analytical solutions of the semi-infinite members captures the characteristics of power flow between members when the

members demonstrate an equal amount of coupling between their normal modes. If large differences exist in the power flow due to the distinct resonant behavior of the short members then the power transfer characteristics cannot be captured properly from analytical solutions of semi-infinite members.

In the past, conventional finite element models have been employed in order to determine the SEA coupling loss factors [18–23] or the EFEA power transfer coefficients [14] instead of the analytical solutions of semi-infinite members. The rationale in these developments was to employ conventional FEA since they can capture the coupling mechanism when the connection between members presents a complexity that cannot be accounted by the analytical solutions of semi-infinite members. An approach based on creating a statistical Green kernel for a boundary element formulation for assembled rods and beams in the mid-frequency range has been presented [24]. The statistical Green kernel is constructed based on random mechanical constants. The fundamental solution is then considered as a random function. A direct boundary element approach is employed to achieve numerical solution. Examples of analyzing a single rod, two co-linear rods, and a single beam were presented [24].

The concept of combining an FEA and an SEA formulation for developing a hybrid approach has been presented [25]. The lack of compatibility at the joint between the SEA variables and the FEA variables became a main issue. An optimization routine was developed to approximate the compatibility at the joint between the SEA and the FEA variables. Recently, another hybrid approach based on coupling FEA and SEA methods has been presented for rod elements [26]. The method was based on utilizing FEA to compute the low-frequency global modes of a system and SEA to represent the high-frequency local modes of each subsystem. The low-frequency global modal degrees of freedom were coupled to the high-frequency local modal degrees of freedom. Assumptions of weak coupling between the subsystems, weak stiffness coupling between local and global degrees of freedom, and rain-on-the-roof type of excitation were made. Also an implicit assumption was made that it was possible to readily identify the global and the local modes of a system. The validation was based on an example of two co-linear rod elements [26].

In previous work, a hybrid FEA formulation was presented for mid-frequency vibration analysis of co-linear beam systems that contain one type of energy [27–29]. The development was based on coupling conventional FEA models of short members to EFEA models of long members. Only one flexural wave existed in the system. External excitation was considered to be applied either on a long or a short member. The joints between long and short members were modelled by combining analytical solutions of semi-infinite members that represent the long members to FEA numerical models for the short members. Power transfer coefficients that include the resonant and damping characteristics of the short members, and relationships between the EFEA and FEA primary variables at the joints were derived. A major advantage offered from the wave-based formulation of the EFEA is the distinction between the energy (and the power) associated with waves travelling towards and away from a joint. At a joint between a long and a short member only the energy associated with the impinging wave contributes to the excitation of the short member. Thus, when multiple members are connected together, effects of strong coupling, power reinjection [16], indirect power flow [30], and power reradiation [31] can be captured correctly by

the hybrid finite element solution [29]. When excitation was applied on a short member, an iterative solution process was formulated for solving simultaneously the FEA system of equations, the EFEA system of equations, and the system of interface equations between short and long members.

Since analytical wave solutions or a spectral analysis method [32] are available for analyzing beams and rods connected together, the main interest of this paper is not to develop yet another technique for the analysis of such systems. Instead, the main objective is to pursue fundamental research for further developing the hybrid FEA by extending the completed basic hybrid FEA formulation [27–29] to systems that contain two types of energy. Beams connected at an arbitrary angle in a two-dimensional space constitute an appropriate test-bed for such development because they exhibit two types of energy while their behavior can be computed analytically. Therefore, the new hybrid FEA development can be validated through comparison with analytical results. In beams connected at an arbitrary angle in a two-dimensional space, both longitudinal and bending waves are generated in the system when an external excitation is applied on the bending degrees of freedom. Since longitudinal wavelengths are considerably longer than bending wavelengths, the frequency range where a beam contains a large number of bending wavelengths and a small number of longitudinal wavelengths comprises the mid-frequency range that is considered in this paper. The bending vibration of a beam is considered as a long member and the longitudinal vibration of the same beam as a short member. Long members exhibit high modal overlap, therefore since their natural frequencies are closely spaced they demonstrate similar behavior at different frequencies. Due to the small length of the waves with respect to the dimension of the members, the space averaged over a wavelength and time averaged over a period energy density presents a small variation with space and provides meaningful information about the state of vibration of the long member. The energy variable can be converted into velocity, displacement, acceleration, strain, and stress according to Ref. [8, Table 7.1]. Short members present low modal overlap and their behavior varies significantly with frequency since their natural frequencies are spaced far apart in the frequency domain. In addition, due to the long wavelengths in the short members, the vibration varies significantly with respect to the location within the member. For the same beam, the bending behavior is modelled by EFEA and the longitudinal behavior by FEA. Connections between different beams are characterized as joint locations and they comprise the areas where there is interaction between bending and longitudinal motion. The joints between long and short members are modelled by combining analytical solutions of semi-infinite members that represent the long members, to FEA numerical models for the short members. Two sets of data are produced from the coupling process. The first set is comprised of power transfer coefficients for each EFEA member at a joint with the short members. The computed power transfer coefficients capture the resonant effects of the short members and the damping that can be present in the short members. The second set of data is comprised of relationships between the primary variables of the EFEA model and the primary variables of the FEA model at a joint between long and short members. Only the energy associated with the impinging waves from the long members to the joint defines the excitations on the short members. Numerical solutions of the new hybrid FEA formulation are compared successfully to analytical solutions for several systems of beams connected at an angle in a two-dimensional space.

2. Background on EFEA

In this paper, the EFEA is utilized for modelling the bending behavior of the beams, therefore, a brief overview of the method is presented. In EFEA, the space and time averaged energy density constitutes the primary variable of the formulation [9–14,33]. The governing differential equation associated with one of the bending degrees of freedom in a beam is

$$\frac{-c_g^2}{\eta\omega}\frac{\mathrm{d}^2\langle \underline{e}\rangle}{\mathrm{d}x^2}+\eta\omega\langle \underline{e}\rangle=\underline{Q}_{in}, \tag{1}$$

where c_g is the group speed of the bending waves, η the hysterisis damping factor, ω the radial frequency, $\underline{Q}_{in}$ the time averaged over a period external input power, and $\langle \underline{e}\rangle$ is the time averaged over a period and space averaged over a wavelength energy density. A finite element approach is employed for solving Eq. (1) numerically, resulting in [33]

$$[E^e]_i\{e^e\}_i=\{F^e\}_i+\{Q^e\}_i, \tag{2}$$

where superscript e indicates element-based quantities, subscript i indicates the ith element, $\{e^e\}_i$ the vector of nodal values for the time and space averaged energy density for the ith element, $[E^e]_i$ the system matrix for the ith element, $\{F^e\}_i$ the vector of external time averaged input power at the nodal locations of the ith element, and $\{Q^e\}_i$ is the vector of internal power flow at the boundary locations of the ith element. In EFEA the term $\{Q^e\}_i$ provides the mechanism for connecting elements together across discontinuities [34]. In the hybrid FEA formulation $\{Q^e\}_i$ provides the mechanism for prescribing the power flow between long and short members.

In EFEA at positions where different members are connected, the energy density is discontinuous. The corresponding boundary between the elements defines a joint location. Therefore, during the assembly of the global system the element matrices do not couple, and the values of the internal power flow at the common node do not overlap to cancel each other. Instead, they remain as variables on the right side of the equation

$$\begin{bmatrix}[E^e]_i & \\ & [E^e]_j\end{bmatrix}\begin{Bmatrix}\{e^e\}_i\\ \{e^e\}_j\end{Bmatrix}=\begin{Bmatrix}\{F^e\}_i\\ \{F^e\}_j\end{Bmatrix}+\begin{Bmatrix}\{Q^e\}_i\\ \{Q^e\}_j\end{Bmatrix}. \tag{3}$$

A special procedure is used for assembling the element matrix into the global matrix equations [33]. A specialized joint element equation is developed to formulate the connection between the discontinuous primary variables at the joint. The values of the power flow at the inter-element nodes corresponding to the two adjacent elements are expressed in terms of the corresponding energy densities [34]:

$$\begin{Bmatrix}Q^e_{ic}\\ Q^e_{jc}\end{Bmatrix}=[J]^i_j\begin{Bmatrix}e^e_{ic}\\ e^e_{jc}\end{Bmatrix}, \tag{4}$$

where subscript c indicates the common node between elements i and j, and $[J]_j^i$ is the joint matrix expressing the mechanism of power transfer between elements i and j. The coefficients of the joint matrix are computed from power transfer coefficients. Introducing Eq. (4) into Eq. (3) results in

$$\left(\begin{bmatrix} [E^e]_i & \\ & [E^e]_j \end{bmatrix} + [JC]_j^i \right) \begin{Bmatrix} \{e^e\}_i \\ \{e^e\}_j \end{Bmatrix} = \begin{Bmatrix} \{F^e\}_i \\ \{F^e\}_j \end{Bmatrix}, \tag{5}$$

where $[JC]_j^i$ is the joint matrix comprising the coefficients of $[J]_j^i$ positioned in the appropriate locations.

3. Hybrid FEA formulation for beams connected at an arbitrary angle

The bending vibration in the beams is modelled by the EFEA formulation and the longitudinal vibration is modelled with conventional FEA. The resonant behavior exhibited by the beams in the longitudinal direction is captured by the FEA formulation. The coupling between bending and longitudinal vibration is created at locations where the beams are connected at non-zero angles. A hybrid joint formulation is developed in order to capture the relationships between the EFEA and FEA primary variables at the joints, and in order to derive power transfer coefficients that include the resonant and damping behavior exhibited by the beams in the longitudinal direction. The power transfer coefficients computed from the hybrid joint formulation are incorporated in the EFEA solution. Relationships between the EFEA and FEA primary variables at the joints are also derived by the hybrid joint formulation. The excitation applied on the longitudinal degrees of freedom from the bending vibration can be determined from the relationships between the EFEA and FEA primary variables and from the EFEA solution. The longitudinal vibration of the beams can be computed by the FEA system of equations once the distribution of the bending energy density has been determined by the EFEA. The bending energy density at the joints along with the relationships between EFEA and FEA primary variables at the joints evaluates the appropriate boundary conditions for the FEA computations.

3.1. Condensation of FEA system of equations

A finite element model is utilized for computing the longitudinal vibration of the beams. The FEA system of equations for the longitudinal behavior of all the beams inter-connected together can be written in matrix form as

$$\lfloor -\omega^2[M] + \mathrm{i}\omega[C] + [K] \rfloor \{u\} = \{R\} \Rightarrow [ST]\{u\} = \{R\}, \tag{6}$$

where $[M], [C], [K]$ is the mass, damping, and stiffness matrix, respectively, $\{u\}$ the displacement of longitudinal vibration in a global two-dimensional system, $[ST]$ the global structural system

matrix including the mass, damping, and stiffness effects, and $\{R\}$ is the vector of reaction forces and moments imposed by supports or external excitation.

By considering two beams connected at each joint location, Eq. (6) can be partitioned into the global degrees of freedom at each joint, the global degrees of freedom at the edges of the system, and all the remaining internal global degrees of freedom:

$$\begin{bmatrix} [ST_{11}] & [ST_{12}] \\ [ST_{21}] & [ST_{22}] \end{bmatrix} \begin{Bmatrix} \begin{Bmatrix} u_x^1 \\ u_y^1 \\ \bullet \\ \bullet \\ \bullet \\ u_x^i \\ u_y^i \\ \bullet \\ \bullet \\ \bullet \\ u_x^M \\ u_y^M \\ u_x^{b1} \\ u_y^{b1} \\ u_x^{b2} \\ u_y^{b2} \end{Bmatrix} \\ \{u_2\} \end{Bmatrix} = \begin{Bmatrix} \begin{Bmatrix} F_x^1 \\ F_y^1 \\ \bullet \\ \bullet \\ \bullet \\ F_x^i \\ F_y^i \\ \bullet \\ \bullet \\ \bullet \\ F_x^M \\ F_y^M \\ F_x^{b1} \\ F_y^{b1} \\ F_x^{b2} \\ F_y^{b2} \end{Bmatrix} \\ \{F_2\} \end{Bmatrix} \Rightarrow \begin{bmatrix} [ST_{11}] & [ST_{12}] \\ [ST_{21}] & [ST_{22}] \end{bmatrix} \begin{Bmatrix} \{u_1\} \\ \{u_2\} \end{Bmatrix} = \begin{Bmatrix} \{F_1\} \\ \{F_2\} \end{Bmatrix}, \quad (7)$$

where u_x^i, u_y^i is the longitudinal degrees of freedom in the global x and y directions at the ith joint location, M the total number of joint locations in the system, superscripts $b1$ and $b2$ indicate the two outer edges in the system, $\{u_2\}$ indicates all the remaining internal global degrees of freedom, F_x^i, F_y^i the forces in the global x and global y directions at the jth joint location, and subscript 2 indicates the global internal degrees of freedom. The displacement vector and the force vector are rewritten in a condensed form by grouping together all the global degrees of freedom at the joints and at the two outer boundaries of the system, and by representing the new group of global degrees of freedom with subscript 1. Since it is considered that no external excitation is applied on the longitudinal degrees of freedom, $\{F_2\} = \{0\}$.

From the lower part of Eq. (7), $\{u_2\}$ can be expressed in terms of $\{u_1\}$ and then substituted in the upper part of the equation. This condensation process results in

$$[S]\begin{Bmatrix} u_x^1 \\ u_y^1 \\ \bullet \\ \bullet \\ \bullet \\ u_x^M \\ u_y^M \\ u_x^{b1} \\ u_y^{b1} \\ u_x^{b2} \\ u_y^{b2} \end{Bmatrix} = \begin{Bmatrix} F_x^1 \\ F_y^1 \\ \bullet \\ \bullet \\ \bullet \\ F_x^M \\ F_y^M \\ F_x^{b1} \\ F_y^{b1} \\ F_x^{b2} \\ F_y^{b2} \end{Bmatrix}, \tag{8}$$

where $[S] = \lfloor [ST_{11}] - [ST_{12}][ST_{22}]^{-1}[ST_{21}] \rfloor$ is the condensed FEA system of equations. The entries of the forcing vector on the right-hand side of Eq. (8) constitute the interaction mechanism between the longitudinal and the bending degrees of freedom at the joints. Eq. (8) is employed for deriving: (i) EFEA power transfer coefficients for the bending waves in the long members including the resonant effects of the short members; (ii) relationships between EFEA and FEA primary variables at the joints.

3.2. Derivation of EFEA power transfer coefficients at joints between long and short members

In order to derive the EFEA power transfer coefficients at the joints, analytical equations representing the bending behavior of semi-infinite beams are coupled with the global longitudinal FEA degrees of freedom at the joints. A separate computation is required by considering a wave impinging from each long member at each joint. One semi-infinite member is utilized for representing the beam where the impinging wave is applied, and one semi-infinite member is employed for representing every other beam in the system where a bending wave is transmitted. A global system of equations is derived based on compatibility conditions between the bending degrees of freedom of the semi-infinite members at the joints and the global longitudinal FEA degrees of freedom at the joint. The termination boundary conditions at the two ends of the system of the inter-connected longitudinal degrees of freedom are also taken into account. The analytical solution of the semi-infinite member that carries the incident and the reflected waves is

$$W_n^i(z,t) = w_n^i(z)\mathrm{e}^{\mathrm{i}\omega t} = [A_n^i \mathrm{e}^{-\mathrm{i}k_n^i z} + C_n^i \mathrm{e}^{\mathrm{i}k_n^i z} + D_n^i \mathrm{e}^{k_n^i z}]\mathrm{e}^{\mathrm{i}\omega t}, \tag{9}$$

where z is the co-ordinate in the local system for the semi-infinite member with origin at the joint, superscript i indicates the joint where the incident wave is impinging, subscript n indicates the semi-infinite member that is carrying the impinging and the reflected waves at joint i, A_n^i the amplitude of incident wave, C_n^i the amplitude of farfield reflected wave, and D_n^i is the amplitude of

nearfield reflected wave. The bending wave number can be obtained by the equation

$$k_n^i = \left[\frac{\omega^2 \rho_n^i S_n^i}{E_n^i I_n^i}\right]^{1/4}, \tag{10}$$

where ρ is the density, S the cross-sectional area, and EI the bending rigidity. The analytical solution of the semi-infinite members that carry the transmitted waves is

$$W_m^j(z,t) = w_m^j(z)e^{i\omega t} = [A_m^j e^{-ik_m^j z} + B_m^j e^{-k_m^j z}]e^{i\omega t}, \tag{11}$$

where superscript j indicates the jth joint, subscript m indicates a semi-infinite member that is carrying the transmitted wave at joint j, A_m^j the amplitude of the farfield transmitted wave, B_m^j the amplitude of the nearfield transmitted wave. The bending wave number k_m^j is evaluated from an equation similar to Eq. (10) by appropriately replacing subscript n with m and superscript i with j. The amplitude of the reflected wave and the amplitudes of all the transmitted waves constitute the unknown variables. The system of equations for the hybrid joint allows to express the unknown variables in terms of the amplitude of the incident wave. Then, the power associated with the farfield impinging, reflected, and transmitted waves can be computed and the power transfer coefficients can be evaluated [27–29].

The total number of unknown variables for each computation of power transfer coefficients is equal to the summation of the global longitudinal FEA degrees of freedom at all the joints ($2M$), the amplitudes of the nearfield and the farfield components of the transmitted waves carried by all the semi-infinite members at all the joints ($2M$), the amplitudes of the near- and farfield components of the reflected wave carried by the semi-infinite member that contains the impinging wave (2), and the longitudinal degrees of freedom at the two outer boundaries of the FEA model (2). Therefore, the total number of unknown variables is $(4M+4)$. Each computation of power transfer coefficients is associated with an impinging wave at a joint. There are four compatibility conditions at every joint where a semi-infinite member carrying a transmitted wave is attached. The equilibrium of forces in the two global directions are

$$F_x^j - F_{bm}^j \sin\theta_m^j = 0, \qquad F_y^j + F_{bm}^j \cos\theta_m^j = 0, \tag{12}$$

where F_x^j, F_y^j is the forces of the FEA formulation of the longitudinal degrees of freedom expressed in the global x and y directions (also defined in Eq. (8)), superscript j indicates the jth joint, θ the angle defining the orientation of each member connected at the jth joint with respect to the global x-axis and F_{bm}^j is the shear force associated with the bending wave transmitted in the semi-infinite member of the jth joint. The compatibility between the longitudinal and the bending displacements at each joint in the two global directions can be stated as

$$u_x^j - w_{bm}^j \sin\theta_m^j = 0, \qquad u_y^j + w_{bm}^j \cos\theta_m^j = 0, \tag{13}$$

where w_{bm}^j is the displacement of the transmitted bending wave at the edge of the semi-infinite member attached to joint j.

For the joint i where a semi-infinite member carrying the impinging wave is attached the equilibrium of forces and compatibility of displacement conditions become

$$\begin{aligned} &F_x^i - F_{bm}^i \sin\theta_m^i - F_{bn}^i \sin\theta_n^i = 0, \qquad F_y^i + F_{bm}^i \cos\theta_m^i - F_{bn}^i \sin\theta_n^i = 0, \\ &u_x^i - w_{bm}^i \sin\theta_m^i - w_{bn}^i \sin\theta_n^i = 0, \qquad u_y^i + w_{bm}^i \cos\theta_m^i + w_{bn}^i \cos\theta_n^i = 0, \end{aligned} \tag{14}$$

where F_{bn}^{i} is the shear force associated with the impinging bending wave, and w_{bn}^{i} the displacement of the impinging bending wave at the edge of the semi-infinite member attached to joint i.

In addition, due to the presence of two semi-infinite members at joint i (one carrying the impinging and one carrying the transmitted wave), two more equations can be stated. They originate from equilibrium of moments and continuity of slope at the joint:

$$M_{bm}^{i} = M_{bn}^{i}, \qquad \frac{\mathrm{d}w_{bm}^{i}}{\mathrm{d}z} = \frac{\mathrm{d}w_{bn}^{i}}{\mathrm{d}z}, \tag{15}$$

where M_{bm}^{i}, M_{bn}^{i} are bending moments applied at the edge of the semi-infinite members that carry the transmitted and the impinging bending waves, respectively.

Two boundary conditions imposed as prescribed displacement or prescribed force on the longitudinal degrees of freedom at the two boundaries of the system are also included in the system of the hybrid joint equations. Therefore, the total number of equations is $(4M + 4)$ which is equal to the number of total unknown variables. The shear forces and the bending moments of the impinging and the transmitted waves are expressed in terms of the analytical displacement solutions (Eqs. (9) and (11)). The global forces which are associated with the longitudinal degrees of freedom in Eq. (12), are expressed in terms of the global longitudinal displacements at the joints and the entries of matrix $[S]$ from the condensed finite element system of equations (Eq. (8)). Thus, solution to the final system of equations for the hybrid joint formulation allows to express all the unknown variables in terms of the amplitude of the impinging wave. The amplitudes of the reflected waves are

$$C_{n}^{i} = af_{nn}^{ii} A_{n}^{i}, \qquad D_{n}^{i} = an_{nn}^{ii} A_{n}^{i}, \tag{16}$$

where af_{nn}^{ii}, an_{nn}^{ii} is the coefficients associated with the far- and nearfield reflected wave components propagating on the semi-infinite member that is carrying the impinging wave at the ith joint. The amplitudes of the transmitted waves are

$$A_{m}^{j} = af_{nm}^{ij} A_{n}^{i}, \qquad B_{m}^{j} = an_{nm}^{ij} A_{n}^{i}, \tag{17}$$

where af_{nm}^{ij}, an_{nm}^{ij} is the coefficients associated with the far- and nearfield components of the wave transmitted on the semi-infinite member of the jth joint due to a wave impinging on the ith joint. Finally, the global longitudinal degrees of freedom at each joint can be expressed as

$$u_{x}^{ij} = ax_{n}^{ij} A_{n}^{i}, \qquad u_{y}^{ij} = ay_{n}^{ij} A_{n}^{i}, \tag{18}$$

where ax_{n}^{ij}, ay_{n}^{ij} is the coefficients associated with the global x and y directions at the jth joint due to the incident wave at the ith joint.

The power transmission coefficient τ_{nm}^{ij} represents the amount of power of the mth transmitted wave at the jth joint due to the nth incident wave at the ith joint. The power reflection coefficient r_{nn}^{ii} represents the amount of power reflected back to the semi-infinite member which is carrying the nth incident wave at the ith joint. Only the amplitudes of the farfield terms participate in the calculation of the power transfer coefficients. Hence, τ_{nm}^{ij} can be defined as

$$\tau_{nm}^{ij} = \frac{(q_{tran})_{m}^{j}}{(q_{inc})_{n}^{i}} = \frac{(EI)_{m}^{j}(k_{m}^{j})^{3}\omega|A_{m}^{j}|^{2}}{(EI)_{n}^{i}(k_{n}^{i})^{3}\omega|A_{n}^{i}|^{2}} = \frac{(EI)_{m}^{j}(k_{m}^{j})^{3}}{(EI)_{n}^{i}(k_{n}^{i})^{3}}|af_{nm}^{ij}|^{2}. \tag{19}$$

The reflection coefficient r_{nn}^{ii} can be defined similarly as

$$r_{nn}^{ii} = \frac{(q_{refl})_n^i}{(q_{inc})_n^i} = \frac{(EI)_n^i (k_n^i)^3 \omega |C_n^i|^2}{(EI)_n^i (k_n^i)^3 \omega |A_n^i|^2} = \frac{|C_n^i|^2}{|A_n^i|^2} = |af_{nn}^{ii}|^2. \tag{20}$$

Transmission and reflection coefficients are computed by considering a bending wave impinging from each beam separately.

3.3. Relationship between the EFEA and the FEA primary variables at a joint between long and short members

The derivation of the EFEA power transfer coefficients accounts for the resonant and damping characteristics of the longitudinal degrees of freedom (short members). The constants af_{nm}^{ij} and af_{nn}^{ii} that are directly related to τ_{nm}^{ij} and r_{nn}^{ii}, respectively, are computed from the system of equations of the hybrid joint formulation. The system of equations includes all the resonant and damping characteristics of the FEA matrix of the longitudinal degrees of freedom. Once the power transfer coefficients have been evaluated, the EFEA system of equations is solved and the distribution of the energy density associated with the bending degrees of freedom is computed for all the beams. The solution for the energy density contains all the resonant and dissipative characteristics of the longitudinal degrees of freedom captured by the power transfer coefficients.

Once the EFEA computations have been completed, the distribution of the energy density can be utilized to evaluate the longitudinal behavior of all the beams. From the EFEA analysis, a value for the bending energy density is computed at the edges of the two beams connected at each joint. The amount of the energy density associated with the impinging wave is identified and utilized to specify the excitation applied on the longitudinal degrees of freedom due to the bending waves. The energy density e_1^i of the left beam at the ith joint can be expressed in terms of a right and a left travelling wave:

$$\begin{aligned} e_1^i &= e_1^{i+} + e_1^{i-} = e_1^{i+} + \frac{q_1^{i-}}{c_{g1}^i S_1^i} = e_1^{i+} + \frac{1}{c_{g1}^i S_1^i}[r_{11}^{ii} q_1^{i+} + \tau_{21}^{ii} q_2^{i-}] \\ &= (1 + r_{11}^{ii}) e_1^{i+} + \frac{c_{g2}^i S_2^i}{c_{g1}^i S_1^i} \tau_{21}^{ii} e_2^{i-}, \end{aligned} \tag{21}$$

where superscripts "+","−" indicate right and left travelling waves, subscripts 1 and 2 indicate the left and the right member connected at the ith joint, and c_{g1}^i, c_{g2}^i the bending group speeds of the left and the right members at the ith joint. In a similar manner, the energy density of the right beam at the ith joint can be expressed as

$$e_2^i = \frac{c_{g1}^i S_1^i}{c_{g2}^i S_2^i} \tau_{12}^{ii} e_1^{i+} + (1 + r_{22}^{ii}) e_2^{i-}. \tag{22}$$

Combining Eqs. (21) and (22) in matrix form results in

$$\begin{Bmatrix} e_1^i \\ e_2^i \end{Bmatrix} = \begin{bmatrix} (1+r_{11}^{ii}) & \dfrac{c_{g2}^i S_2^i}{c_{g1}^j S_1^j}\tau_{21}^{ii} \\ \dfrac{c_{g1}^i S_1^i}{c_{g2}^i S_2^i}\tau_{12}^{ii} & (1+r_{22}^{ii}) \end{bmatrix} \begin{Bmatrix} e_1^{i+} \\ e_2^{i-} \end{Bmatrix} = [E] \begin{Bmatrix} e_1^{i+} \\ e_2^{i-} \end{Bmatrix}. \tag{23}$$

The values for e_1^i and e_2^i are evaluated by the EFEA computations for the long members. In the EFEA analysis, the power transfer coefficients account for the resonant behavior and the dissipation associated with the longitudinal degrees of freedom. The values for e_1^{i+} and e_2^{i-} are computed from Eq. (23) and they are utilized to prescribe the excitation on all the longitudinal degrees of freedom at all the joints. Only the component of the energy density associated with the impinging wave is employed for defining the excitation on the system of the longitudinal degrees of freedom. The values of the energy densities e_1^{i+} and e_2^{i-} are employed for defining the amplitudes of the two bending waves impinging at the ith joint. Each amplitude of the impinging waves provides the excitation in the hybrid joint system of equations. The boundary conditions applied on all the longitudinal degrees of freedom at all the joint locations due to each wave impinging at the ith joint are computed. The excitations applied on the longitudinal system by all the waves impinging at the joints are incoherent since the impinging waves originate from the reverberant field of each long member. The energy density e_n^i of an impinging wave at the ith joint is associated with the amplitude of the corresponding impinging wave as

$$e_n^i = \tfrac{1}{2}\rho_n^i \omega^2 |A_n^i|^2. \tag{24}$$

Eqs. (18) and (24) are employed for developing relationships between the global FEA degrees of freedom at all the joints and the energy density associated with an impinging bending wave at the ith joint.

3.4. System solution

An external input power is considered to be applied on the long members (bending degrees of freedom) as external excitation. The global EFEA system matrix is assembled for all the long members. Power transfer coefficients evaluated from analytical solutions of semi-infinite members and FEA models that represent the longitudinal behavior are utilized for generating coupling matrices between long members. The power transfer coefficients derived by Eqs. (19) and (20) are employed for developing the joint matrices. The power transfer coefficients incorporate the resonant effects and the dissipative characteristics of the longitudinal degrees of freedom in the power transfer mechanism between all the long members. The joint matrices represent the interaction between all the EFEA degrees of freedom at all the joint locations and they include the power transferred among them through the longitudinal degrees of freedom. The EFEA system of equations is solved first, and the distribution of the energy density over all the long members is evaluated. From the values of the bending energy density at each joint the energy density associated with each one of the two impinging bending waves is computed from Eq. (23). For each impinging bending wave, Eqs. (24) and (18) are employed for defining the global longitudinal FEA degrees of freedom at all the joints. The FEA method is employed to solve for all the internal

FEA degrees of freedom $\{{}^{n}u_2^i\}$ due to a bending wave impinging at the ith joint. By taking into account the partitioning and condensation process applied on the FEA system of equations $\{{}^{n}u_2^i\}$ can be computed:

$$\{{}^{n}u_2^i\} = -[ST_{22}]^{-1}[ST_{21}]\begin{Bmatrix} \\ u_x^{i1} \\ u_y^{i1} \\ \bullet \\ \bullet \\ \bullet \\ u_x^{iM} \\ u_y^{iM} \\ u_x^{b1} \\ u_y^{b1} \\ u_x^{b2} \\ u_y^{b2} \end{Bmatrix}, \tag{25}$$

where $\{{}^{n}u_2^i\}$ is the response of the internal FEA degrees of freedom due to excitation originating from an impinging bending wave (superscript n) at the ith joint (superscript i). The bending energy density at the joints originates from the incoherent field of the long members. Thus, the excitations applied on the longitudinal FEA degrees of freedom from all the bending waves impinging at the joints are considered as incoherent. The total response and the energy density distribution over the short members is evaluated by adding up the FEA response $\{{}^{n}u_2^i\}$ computed from each impinging wave on an energy basis. The effects from power reinjected in the long members is accounted in the solution since Eq. (23) includes on the left side terms associated with both reflected power and power transmitted from the other long member [27,29]. The flow chart of the new hybrid FEA formulation is presented in Fig. 1.

4. Validation

The hybrid FEA formulation presented in this work is validated by computing the bending energy (long members) and the longitudinal energy (short members) for two beam configurations and comparing the numerical results to analytical solutions (see Appendix A). The properties of the beams that are utilized in the validation are summarized in Table 1. Variations of two primary configurations of a two-beam (Fig. 2) and a three-beam (Fig. 3) system are analyzed. Free end boundary conditions are considered for all systems. A harmonic force in the transverse direction is applied at the left free end of each system. Several configurations of these two systems with variations imposed on the length of certain members are employed in the validation (Table 1). The hybrid results are compared to analytical solutions. In order to simulate in the analytical solution the ensemble average behavior of the bending motion, a 4% variation is introduced in the length

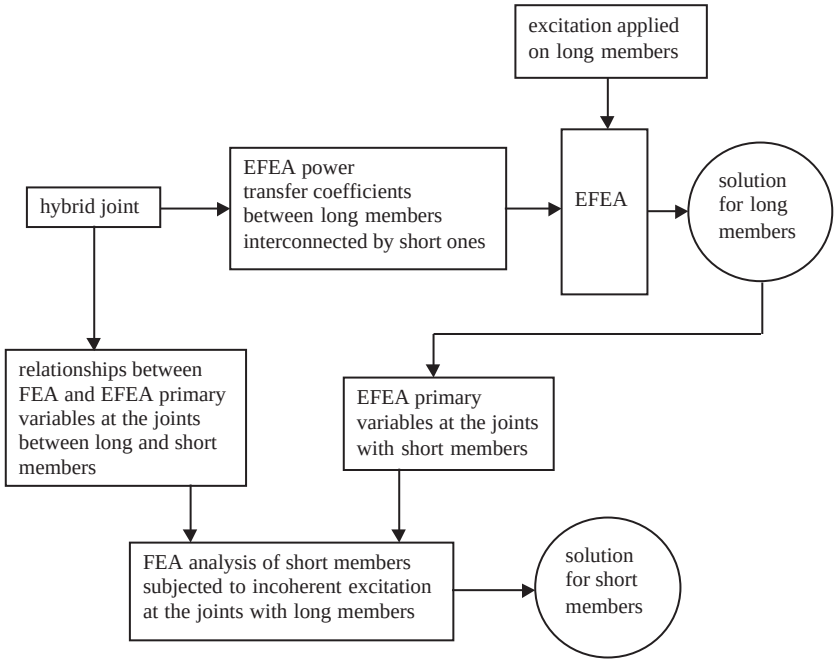

Fig. 1. Flow chart of the hybrid computational process.

Table 1
Properties of beams employed in the validation

		Long beam
Young's modulus of elasticity E (N/m^2)		19.5×10^{10}
Moment of inertia I (m^4)		9.365×10^{-10}
Mass density ρ (kg/m^3)		7,700
Damping factor η		0.02
Cross-sectional area A (m^2)		1.935×10^{-4}
Cross-sectional dimensions width × height (m)		0.0254×0.00762
Length of beams (m)	All beams in two-beam system	3
	All beams in three-beam system	3
	Three-beam system with altered length Left beam-middle beam-right beam	6-3-3

of the beam members [35]. The ensemble of systems incorporates all the effects of uncertainty associated with the long members but it is defined for a specific frequency [16]. In the validation presented in this paper it is preferred to introduce the uncertainty associated with the long members (bending degrees of freedom) through an ensemble of systems rather than frequency averaging in order to better demonstrate in the solution the highly resonant effects of the short members (longitudinal degrees of freedom).

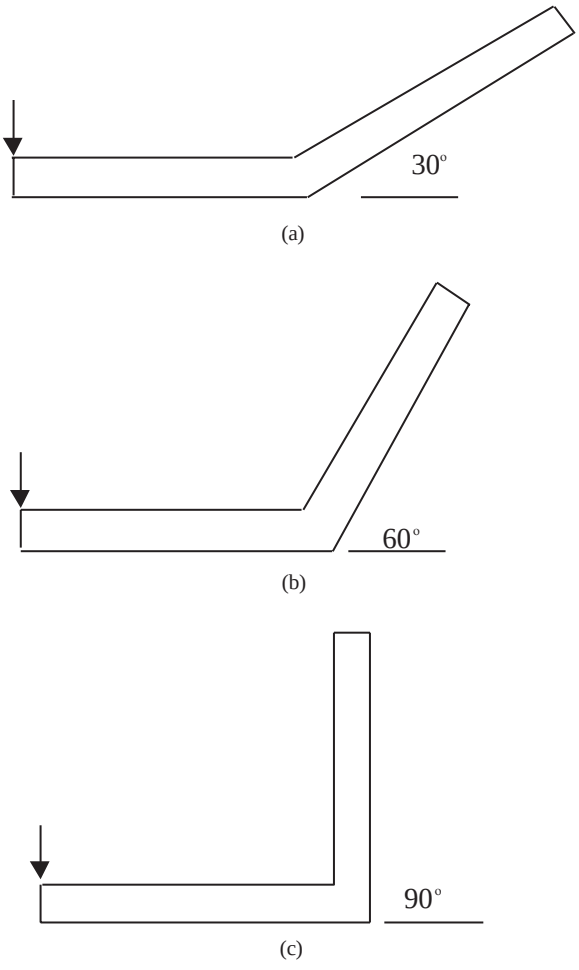

Fig. 2. Two-beam assembly utilized in the validation: (a) 30°; (b) 60°; (c) 90°.

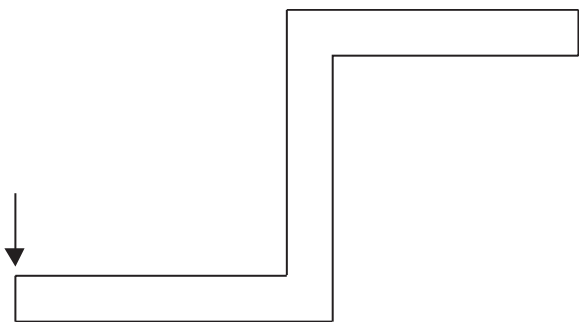

Fig. 3. Three-beam assembly utilized in the validation.

4.1. Two-beam system

Two beams connected at three different angles ($30°, 60°, 90°$) are analyzed first. The analytical solutions for the bending energy density associated with the long members and the longitudinal energy density associated with the short members are presented in Figs. 4–6 for the configurations with $30°, 60°, 90°$ angle, respectively, over an extended frequency range. The results allow to determine the frequency regions where bending waves and longitudinal waves demonstrate comparable energy density. The frequency regions of 625–675 Hz for the 30° configuration, 765–855 Hz for the 60° configuration, and 800–880 Hz for the 90° configuration are identified as the frequency ranges where a large amount of energy is associated with the longitudinal motion. Thus, the three identified frequency regions are selected to perform validation analyses for the hybrid FEA method since the longitudinal motion presents resonant behavior in the selected frequency regions. In order to demonstrate the improvement achieved in the numerical solution by the development of the hybrid formulation, the EFEA is utilized as a representative high-frequency approach to model both the bending and the longitudinal behavior of the beams. The EFEA results demonstrate the inherent deficiency of a high-frequency method (EFEA, SEA) when simulating the behavior of a system in the mid-frequency range due to the inability to capture the resonant behavior of the short members (longitudinal degrees of freedom). The hybrid

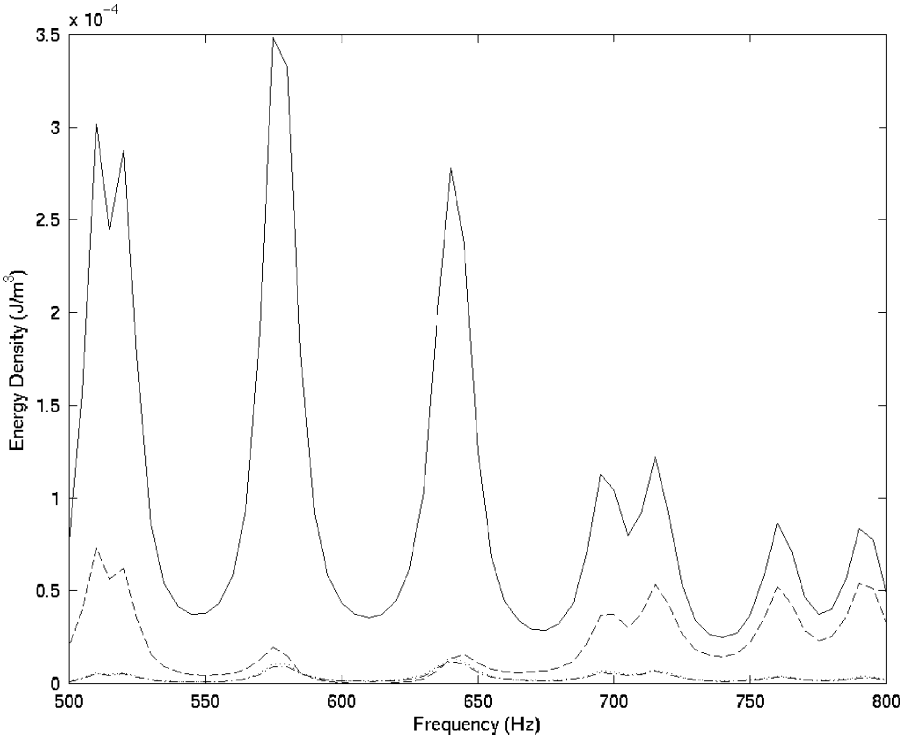

Fig. 4. Analytical averaged bending and longitudinal energy density of two-beam system connected at 30°, 500–800 Hz: ——, analy flexural—left long; - -, analy flexural—right long; · — ·, analy longitudinal—left long; ....., analy longitudinal—right long.

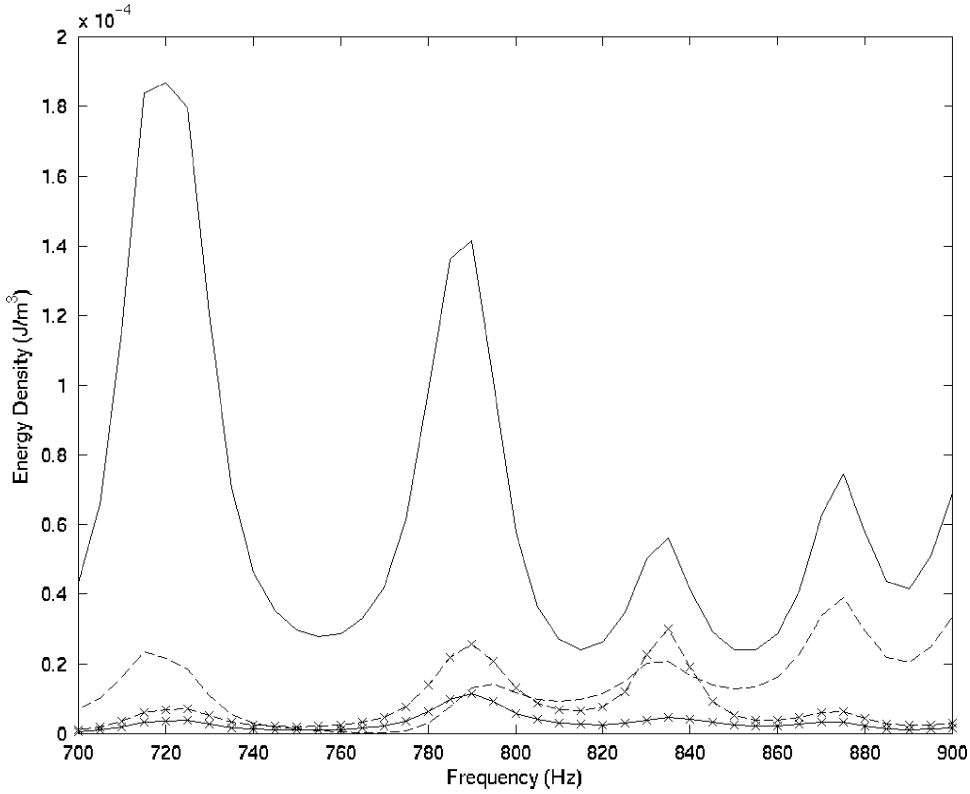

Fig. 5. Analytical averaged bending and longitudinal energy density of two-beam system connected at 60°, 700–900 Hz: ——, analy flexural—left long; - -, analy flexural—right long; —×—, analy longitudinal—left long; —×—, analy longitudinal—right long.

solution constitutes an improvement and the results correlate well with the analytical solution for both the bending and the longitudinal degrees of freedom.

The bending energy, the longitudinal energy, and the total energy of the system calculated by the hybrid FEA, the EFEA, and analytically are presented in Figs. 7–9 for the three configurations connected at $30°, 60°$, and $90°$, respectively. In the energy-based formulations (SEA, EFEA), the primary variables of the energy (total energy stored in each group of similar modes in the SEA, or the energy density associated with each type of wave in the EFEA) are considered to be uncorrelated and the energy variables can be added in order to evaluate the total amount of energy in the system [8,11,13]. The same principle, expressed as continuity of power flow is also utilized for evaluating the power transfer coefficients at a joint between structural members [17]. When computing the power transfer coefficients the power of the impinging wave is considered to be equal to the summation of the power of all the transmitted and reflected waves irrespectively of the wave type. Thus, in the systems analyzed in this paper the total energy of the system is considered equal to the summation of the bending and the longitudinal energy in the system. Since the same amount of input power is defined as excitation in all three solutions, as expected, the results for the total energy in the system are the same for all three methods. The

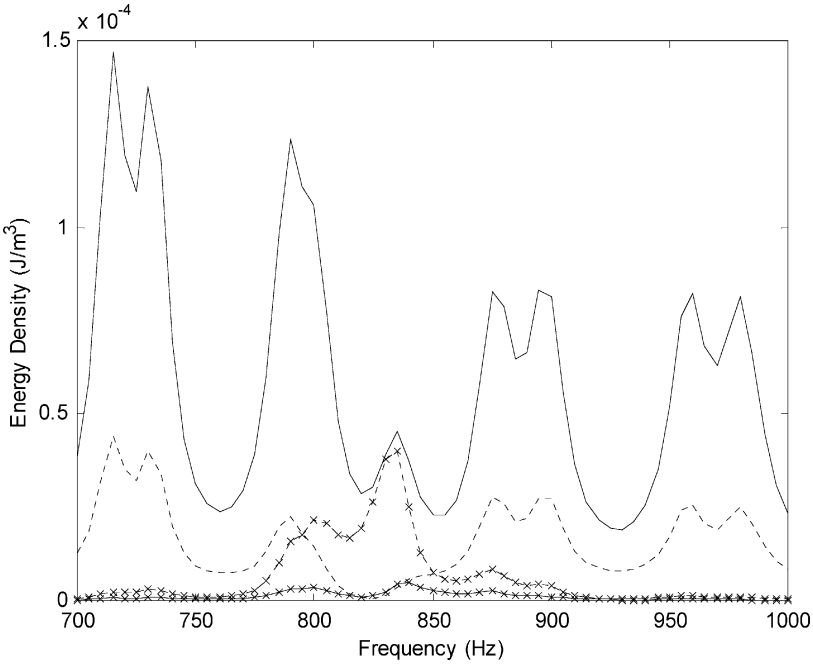

Fig. 6. Analytical averaged bending and longitudinal energy density of two-beam system connected at 90°, 700–1000 Hz: ——, analytical bending—left beam; - - - -, analytical bending—right beam; —×—, analytical longitudinal—left beam; —×—, analytical longitudinal—right beam.

differentiation in the results occurs in the predicted distribution of bending and longitudinal energy in the members. The EFEA does not capture the resonant behavior of the longitudinal degrees of freedom and it predicts that almost the entire amount of energy is stored in the bending degrees of freedom. In addition, the EFEA predicts a very small amount of energy associated with the longitudinal motion. The hybrid FEA captures correctly the highly resonant behavior of the longitudinal degrees of freedom, and the results are identical with the analytical solution. In particular, in the 90° configuration it can be observed from Fig. 9 that between 825 and 835 Hz the longitudinal and the bending energies obtain approximately the same values. This event is correctly predicted by the hybrid FEA and severely missed by the high-frequency EFEA solution. In addition, it can also be observed from Figs. 7–9, that the percentage of energy converted to longitudinal energy increases as the angle of connection between the two beams reaches 90°. This is expected because at 90° more bending energy can be converted into longitudinal energy between the two members [36].

The average energy density of a member is computed by dividing the total energy of the member by its volume. The average energy density of a member is utilized as a measure for the overall behavior at a particular frequency. Results for the bending and the longitudinal energy density are presented in Figs. 10–12 for all three configurations. The good correlation between the hybrid FEA and the analytical solution demonstrates that the hybrid FEA formulation captures accurately the power transfer mechanism between long and short members, the resonant behavior of the short members, and the coupling between EFEA and FEA solutions for the long and short

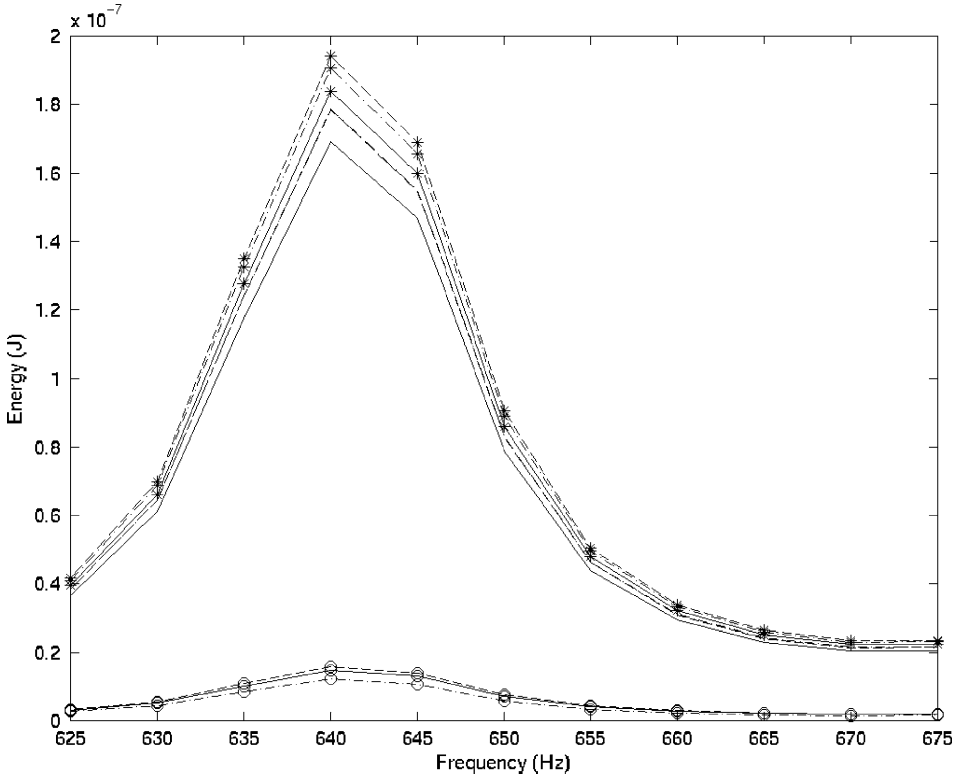

Fig. 7. Analytical, hybrid, and EFEA results for bending, longitudinal, and total energy of the two-beam system connected at 30°, 625–675 Hz: —✳—, analy—total; —✳—, hybrid—total; ✳, EFEA—total; ——, analy—flexural; - -, hybrid—flexural; ···, EFEA—flexural; —○—, analy—longitudinal; —○—, hybrid—longitudinal; ○, EFEA—longitudinal.

members, respectively. Twenty finite elements are utilized in each FEA model for the longitudinal degrees of freedom (short members) and six elements comprise each EFEA model of the bending degrees of freedom (long members). The high-frequency EFEA analysis severely overpredicts the bending energy and underpredicts the longitudinal energy of the system since it does not account for the resonant behavior of the longitudinal degrees of freedom.

4.2. Three-beam system

A system of three beams connected at 90° angle is analyzed (Fig. 3). Excitation is applied at the left end of the system. Analytical results for the bending energy density and the longitudinal energy density are presented in Fig. 13 over an extended frequency range 550–1200 Hz in order to identify a frequency range where the resonant effects of the longitudinal degrees of freedom are prominent. The frequency range 770–850 Hz is selected for all analyses of the three-beam system since resonant behavior is demonstrated in the longitudinal degrees of freedom. Results for the bending energy, the longitudinal energy, and the total energy in the system are presented in Fig. 14 for all three methods. Since the same external input power is specified as excitation in all three methods, as expected, all of them demonstrate the same amount of total energy at each frequency.

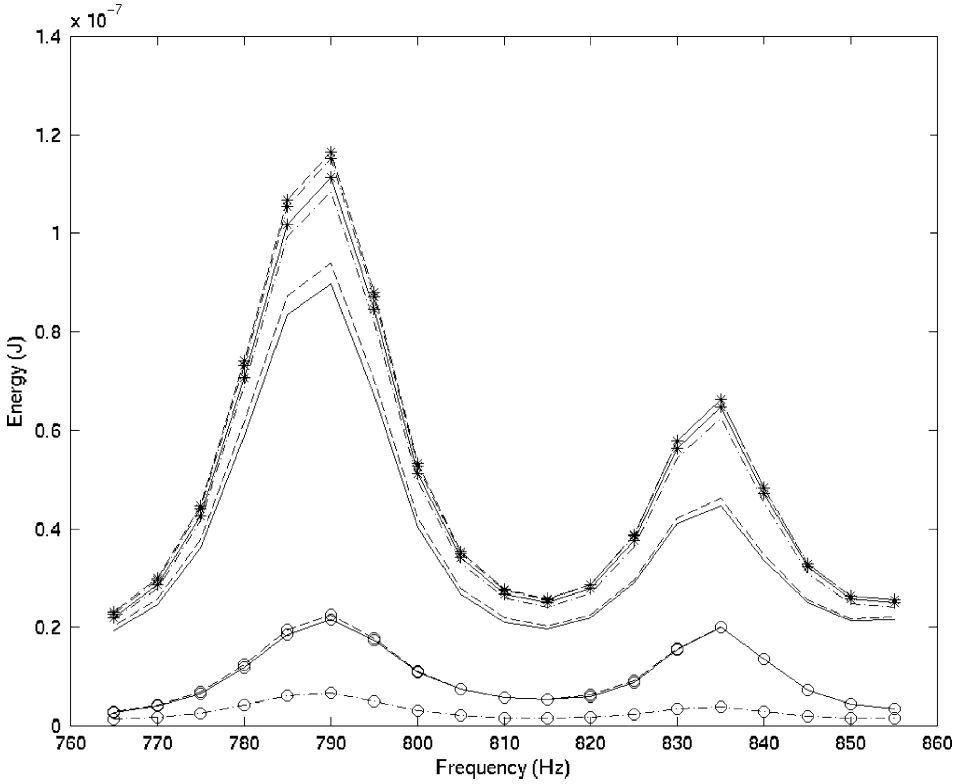

Fig. 8. Analytical, hybrid, and EFEA results for bending, longitudinal, and total energy of the two-beam system connected at 60°, 765–855 Hz: —✳—, analy—total; —✳—, hybrid—total; ✳, EFEA—total; ——, analy—flexural; - -, hybrid—flexural; ·-·, EFEA—flexural; —○—, analy—longitudinal; —○—, hybrid—longitudinal; ○, EFEA—longitudinal.

The dissipated power is proportional to the total energy, therefore, the good agreement observed in Fig. 14 for the total energy validates that dissipation is modelled properly in all three solutions. The distribution of the energy between the bending and the longitudinal degrees of freedom differentiates the hybrid FEA from the EFEA solution. Similar to the two-beam system, the EFEA does not capture the longitudinal resonant behavior of the three-beam system. Thus, it severely underpredicts the longitudinal energy and overpredicts the bending energy. The hybrid FEA provides consistently good results compared to the analytical solution.

Due to the location of the excitation and the configuration of the system, the left beam demonstrates the highest bending energy, and the middle beam demonstrates the highest longitudinal energy. Results for the average bending energy density in the left beam and the average longitudinal energy density in the middle beam are presented in Fig. 15. The agreement between the hybrid and analytical solutions remains good. The EFEA underpredicts the resonant behavior in the longitudinal direction and overpredicts the bending energy level.

The length of the left beam is extended from 3 to 6 m. This modification alters the boundary conditions among the three members, and changes the power transfer coefficients among the long members. Results for the total energy, the bending energy, and the longitudinal energy of the

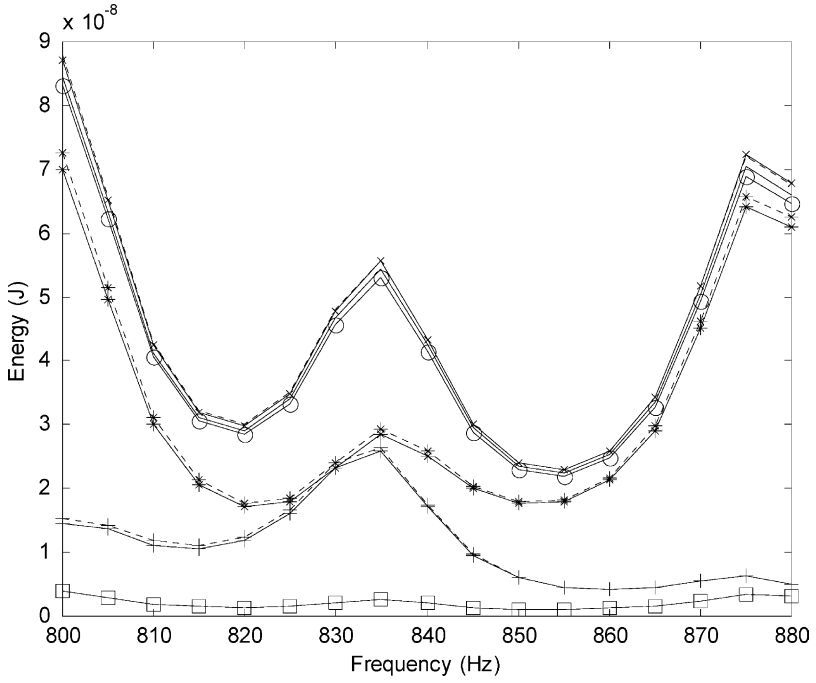

Fig. 9. Analytical, hybrid, and EFEA results for bending, longitudinal, and total energy of the two-beam system connected at 90°, 800–880 Hz: ——, analytical—total; - - -, hybrid—total; —×—, EFEA—total; —✳—, analytical—bending; – ✳—, hybrid—bending; —○—, EFEA—bending; —+—, analytical—longitudinal; – +—, hybrid—longitudinal; —□—, EFEA—longitudinal.

system from the analytical, the hybrid FEA, and the EFEA solutions are presented in Fig. 16. As expected, the energy levels are different than the previous three-beam system. The trends remain the same with the hybrid FEA correlating well to the analytical solution and the EFEA missing the longitudinal resonant effects. Results for the bending energy density in the left beam and the longitudinal energy density in the middle beam are presented in Fig. 17. The hybrid formulation correlates well to the analytical results since it accounts for the power transfer mechanism between long members for the resonant and the energy dissipation effects of the short members. In addition, the hybrid FEA accounts properly for power balance and power reinjection.

5. Conclusions

A basic hybrid FEA formulation for mid-frequency vibration analysis of beams connected at arbitrary angles in a two-dimensional space is presented. Both bending and longitudinal waves propagate in the system. In the mid-frequency range the bending behavior of the beams is considered as incoherent and it is simulated by the EFEA and the longitudinal behavior is considered as resonant and it is simulated by the FEA. Interface conditions between the primary variables of the two formulations are derived at the joints and they constitute the hybrid joint formulation. Power transfer coefficients for the EFEA method that include the resonant and

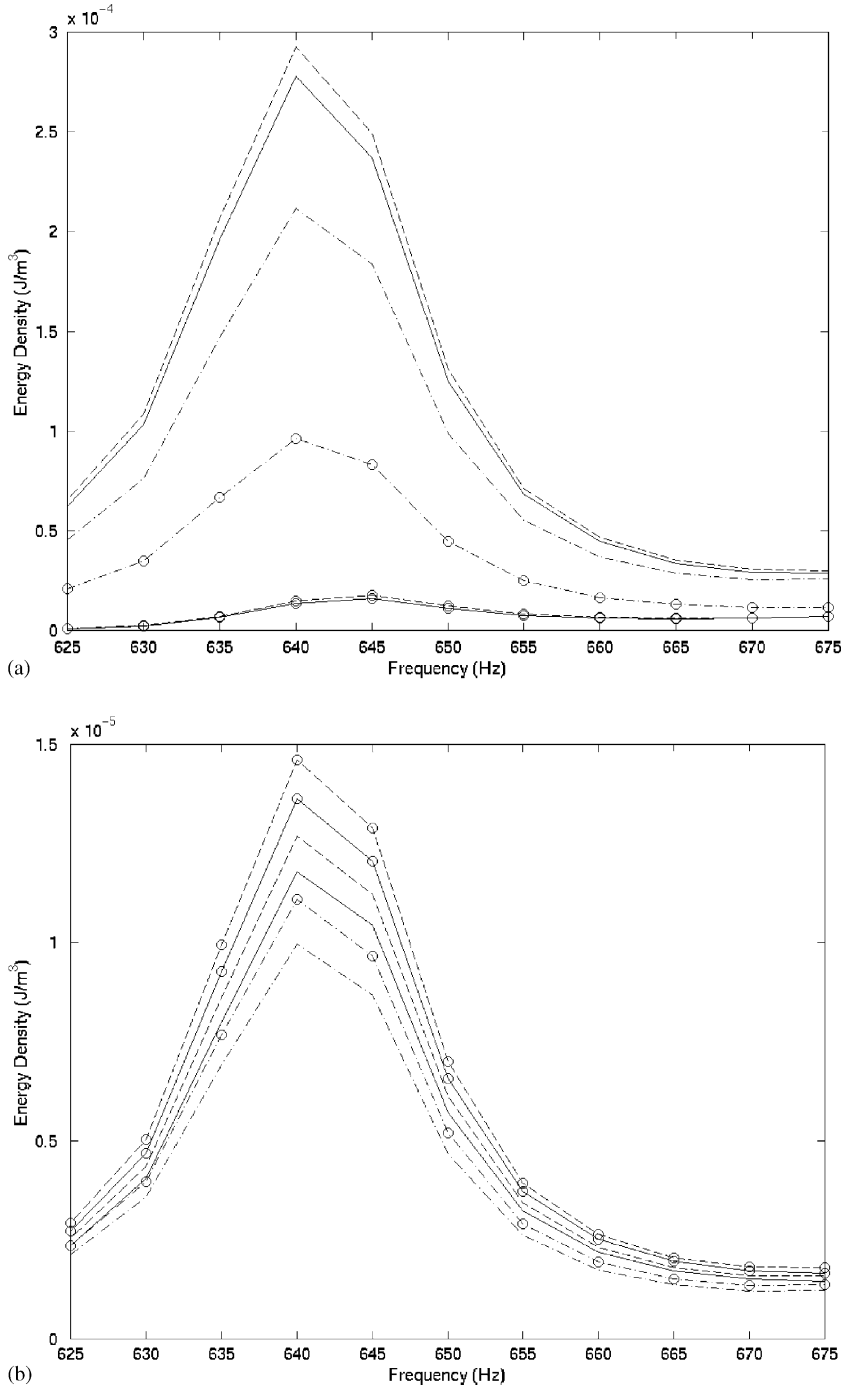

Fig. 10. Analytical, hybrid, and EFEA results for energy density of the two-beam system connected at 30°, 625–675 Hz; (a) bending; (b) longitudinal: ——, analy—left; - -, hybrid—left; ·-·, EFEA—left; —⊖—, analy—right; —○—, hybrid—right; ⊖, EFEA—right.

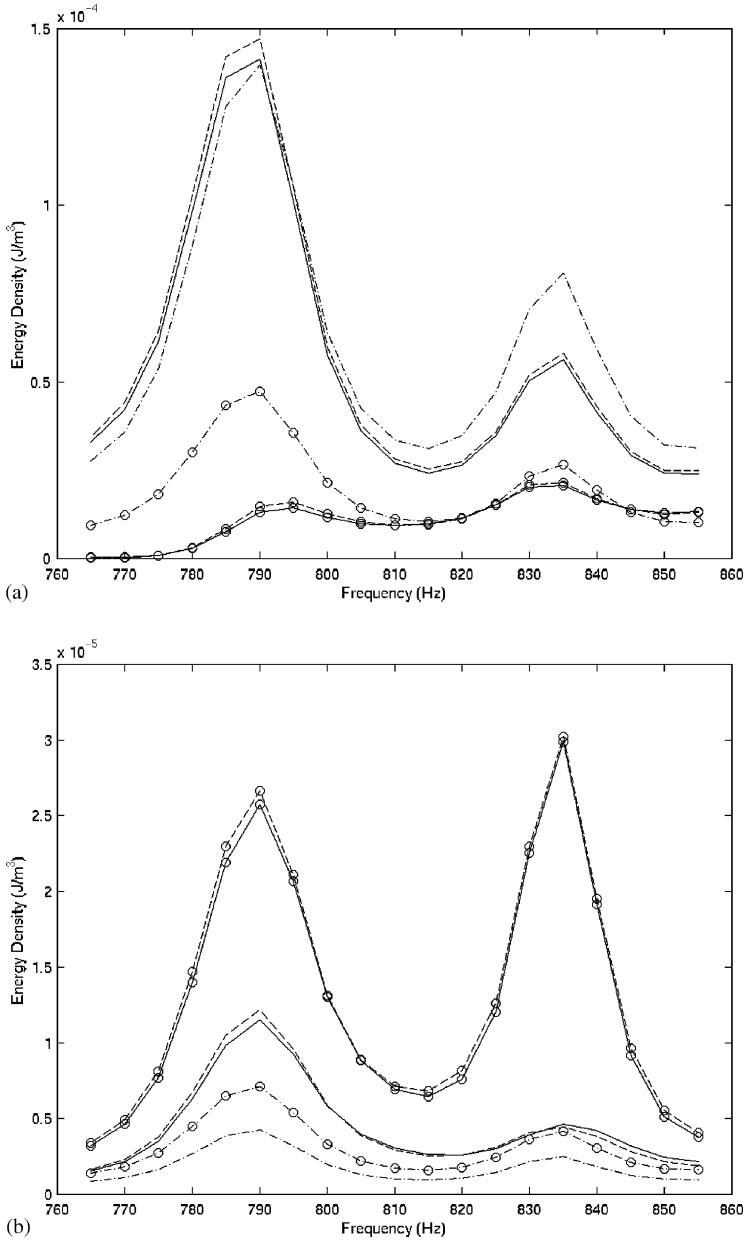

Fig. 11. Analytical, hybrid, and EFEA results for energy density of the two-beam system connected at 60°, 765–855 Hz; (a) bending; (b) longitudinal: ——, analy—left; - -, hybrid—left; ·--·, EFEA—left; —○—, analy—right; –○–, hybrid—right; ·○·, EFEA—right.

dissipative characteristics of the longitudinal vibration are derived from the hybrid joint formulation. The external excitation is considered to be applied on the bending degrees of freedom. The EFEA system of equations is solved first and the distribution of the bending energy over all the beams is computed. The interface conditions between the EFEA and FEA primary

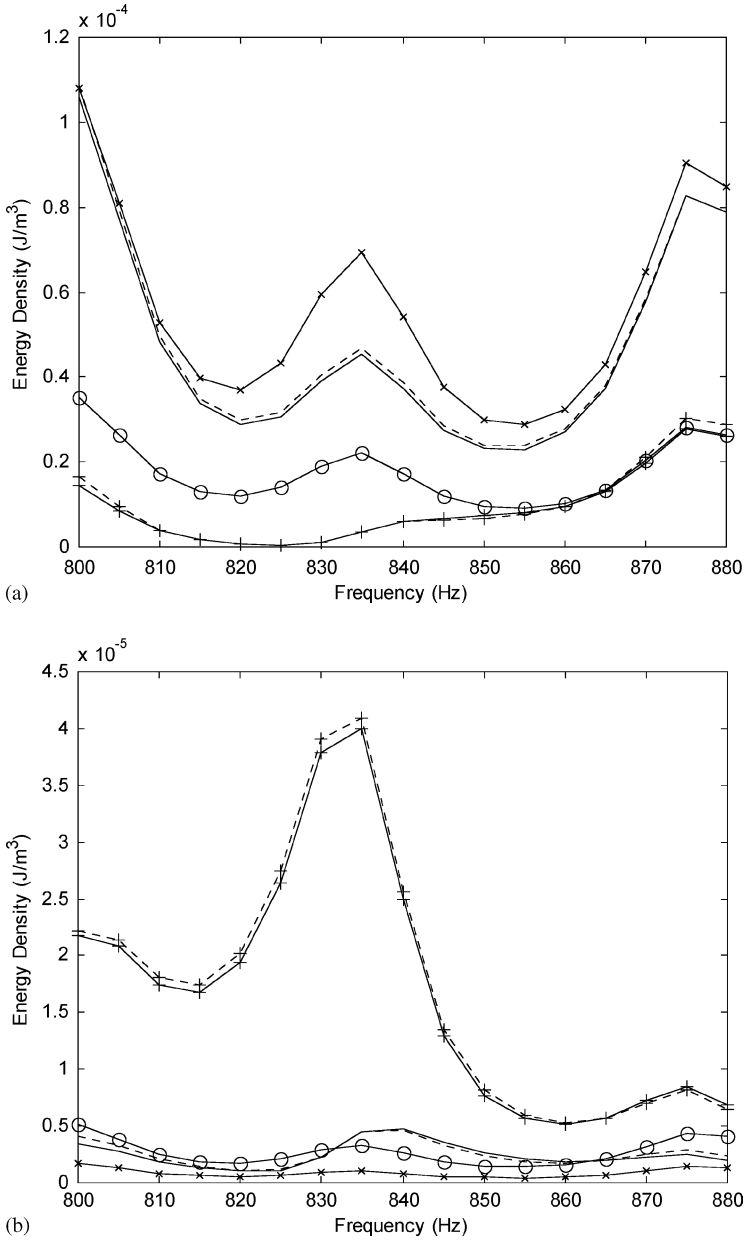

Fig. 12. Analytical, hybrid, and EFEA results for energy density of the two-beam system connected at 90°, 800–880 Hz; (a) bending; (b) longitudinal: ——, analytical—left beam; - - -, hybrid—left beam; —×—, EFEA—left beam; ——+——, analytical—right beam; – – +—, hybrid—right beam; —○—, EFEA—right beam.

variables are employed for deriving the excitation imposed on the longitudinal FEA degrees of freedom from the distribution of the bending energy. Several configurations of a two-beam and a three-beam system are analyzed and results are compared between an analytical solution, the hybrid FEA, and the high-frequency EFEA solution. The hybrid FEA method presents

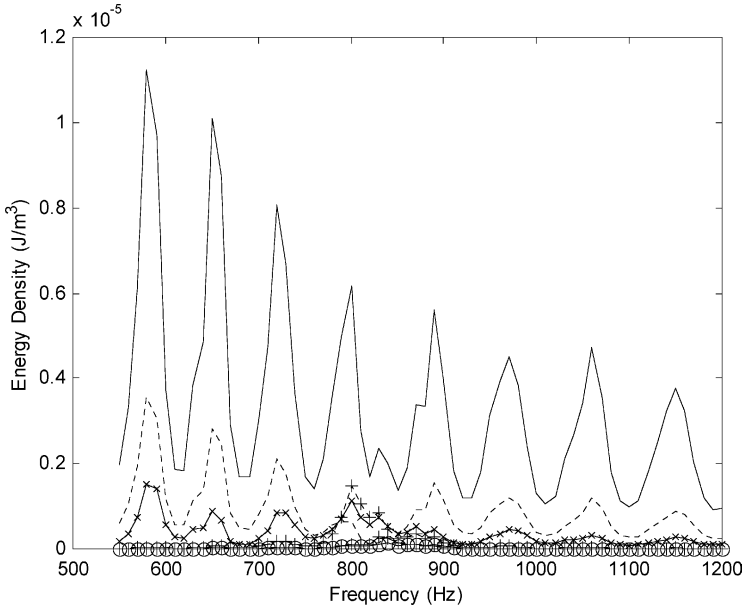

Fig. 13. Analytical averaged bending and longitudinal energy density of three-beam system, 550–1200 Hz: ——, analytical bending—left beam; - - -, analytical bending—middle beam; –×–, analytical bending—right beam; —+—, analytical longitudinal—left beam; – +–, analytical longitudinal—middle beam; –○–, analytical longitudinal—right beam.

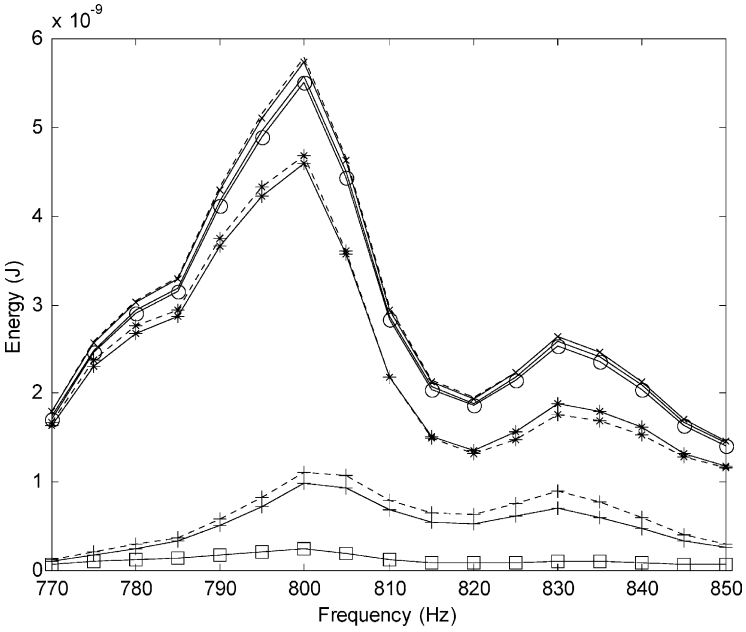

Fig. 14. Analytical, hybrid, and EFEA results for bending, longitudinal, and total energy of the three-beam system, 770–850 Hz: ——, analytical—total; - - -, hybrid—total; –×–, EFEA—total; ✳, analytical—bending; – ✳–, hybrid—bending; –○–, EFEA—bending; —+—, analytical—longitudinal; – +–, hybrid—longitudinal; –□–, EFEA—longitudinal.

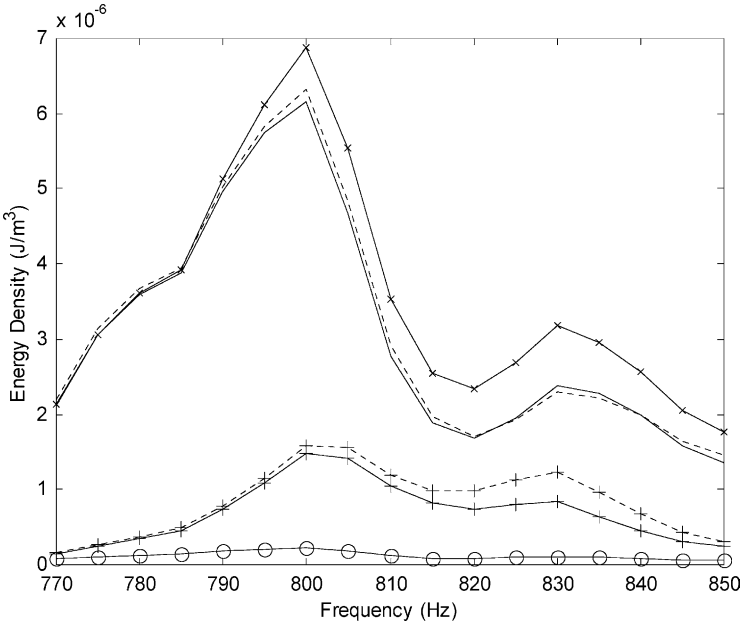

Fig. 15. Analytical, hybrid, and EFEA results for bending, and longitudinal energy density of the three-beam system, 770–850 Hz: ——, analytical bending—left beam; - - - -, hybrid bending—left beam; —×—, EFEA bending—left beam; —+—, analytical longitudinal—middle beam; – +—, hybrid longitudinal—middle beam; —○—, EFEA longitudinal—middle beam.

consistently good agreement with the analytical solution. The EFEA cannot predict accurately the resonant behavior of the system since the resonant characteristics of the longitudinal degrees of freedom are not included in the high-frequency EFEA solution.

Acknowledgements

This research was sponsored by the Automotive Research Center (ARC) established at The University of Michigan, Ann Arbor, by the US Army/Tank-Automotive and Armaments Command (TACOM).

Appendix A. Analytical solution

The mid-frequency approach (hybrid FEA) presented in this paper is validated through comparison with an analytical solution. The analytical solution for systems of beams connected at an arbitrary angle is computed by a MATLAB code. First, the displacement solutions for the bending and the longitudinal degrees of freedom are considered:

$$W_L(x_L,t) = (A_L e^{-ik_L x_L} + B_L e^{-k_L x_L} + C_L e^{ik_L x_L} + D_L e^{k_L x_L}) e^{i\omega t}, \tag{A.1}$$

$$W_S(x_S,t) = (G_S e^{-ik_S x_S} + H_S e^{ik_S x_S}) e^{i\omega t}, \tag{A.2}$$

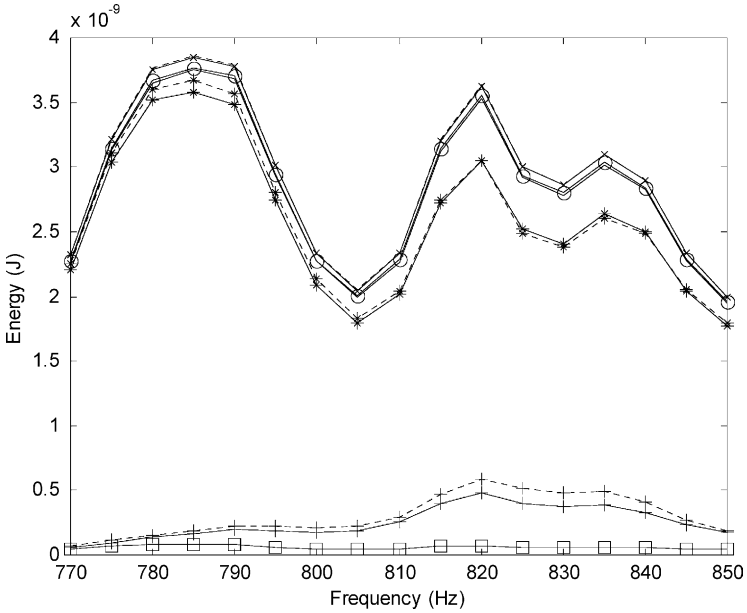

Fig. 16. Analytical, hybrid, and EFEA results for bending, longitudinal, and total energy of the three-beam system with altered length, 770–850 Hz: ——, analytical—total; - - -, hybrid—total; —×—, EFEA—total; —✳—, analytical—bending; – ✳—, hybrid—bending; —○—, EFEA—bending; —+—, analytical—longitudinal; – +—, hybrid—longitudinal; —□—, EFEA—longitudinal.

where subscripts L and S are associated with the long (bending) and the short (longitudinal) members, respectively, $W_L(x_L, t)$ is the analytical transverse displacement solution of a long member (function of x_L and t), A_L the amplitude of the right travelling farfield bending wave, B_L the amplitude of the right travelling nearfield bending wave, C_L the amplitude of the left travelling farfield bending wave, D_L the amplitude of the left travelling nearfield bending wave, k_L the complex flexural wave number of the long member, ω the radial frequency, $W_S(x_S, t)$ the analytical longitudinal displacement solution of a short member (function of x_S and t), G_S the amplitude of the right travelling longitudinal wave, H_S the amplitude of the left travelling longitudinal wave, and k_S the complex longitudinal wave number of the short member. A separate reference system is utilized for each member. The origin is positioned at the left end of each member. The power flow and energy density in the long and the short members are expressed in terms of the corresponding analytical displacement solutions.

The power flow associated with the bending waves is evaluated from the shear force and the bending moment. The power flow associated with the longitudinal waves is evaluated from the axial force. The time averaged power associated with the long and short members is

$$\langle q_L \rangle = \frac{1}{2} E_L I_L \mathrm{Re}\left\{ \frac{\partial^3 W_L}{\partial x_L^3} \left(\frac{\partial W_L}{\partial t} \right)^* - \frac{\partial^2 W_L}{\partial x_L^2} \left(\frac{\partial^2 W_L}{\partial x_L \partial t} \right)^* \right\} \quad \text{for a long member,} \tag{A.3}$$

$$\langle q_S \rangle = \frac{1}{2} E_S S_S \mathrm{Re}\left\{ -\frac{\partial W_S}{\partial x_S} \left(\frac{\partial W_S}{\partial t} \right)^* \right\} \quad \text{for a short member.} \tag{A.4}$$

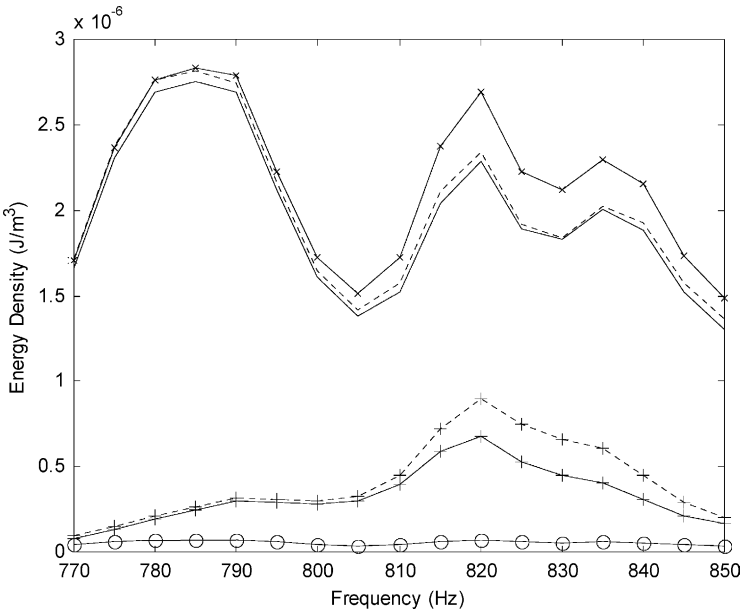

Fig. 17. Analytical, hybrid, and EFEA results for bending, and longitudinal energy density of the three-beam system with altered length, 770–850 Hz: ——, analytical bending—left beam; - - - -, hybrid bending—left beam; –×–, EFEA bending—left beam; —+—, analytical longitudinal—middle beam; – –+–, hybrid longitudinal—middle beam; –○–, EFEA longitudinal—middle beam.

The total bending energy density in a beam is computed as the sum of the potential energy density V_L and the kinetic energy density T_L of the bending waves. The total energy density in a longitudinally vibrating short member is computed as the sum of its potential energy density V_S and kinetic energy density T_S of the longitudinal waves. The time-averaged total energy density solutions for the long and the short members are

$$\langle e_L \rangle = \frac{1}{4}\frac{E_L I_L}{S_L}\left\{\frac{\partial^2 W_L}{\partial x_L^2}\left(\frac{\partial^2 W_L}{\partial x_L^2}\right)^*\right\} + \frac{1}{4}\rho_L\left\{\frac{\partial W_L}{\partial t}\left(\frac{\partial W_L}{\partial t}\right)^*\right\} \quad \text{for a long member,} \tag{A.5}$$

$$\langle e_S \rangle = \frac{1}{4}E_S\left\{\frac{\partial W_S}{\partial x_S}\left(\frac{\partial W_S}{\partial x_S}\right)^*\right\} + \frac{1}{4}\rho_S\left\{\frac{\partial W_S}{\partial t}\left(\frac{\partial W_S}{\partial t}\right)^*\right\} \quad \text{for a short member.} \tag{A.6}$$

Substitution of the displacement solutions (Eqs. (A.1) and (A.2) into Eqs. (A.5) and (A.6) allows to express the time-averaged energy density as

$$\begin{aligned}\langle e_L \rangle = {} & \frac{1}{4}\frac{E_L I_L}{S_L}|k_L^2|^2 \times (-A_L e^{-ik_L x_L} + B_L e^{-k_L x_L} - C_L e^{ik_L x_L} + D_L e^{k_L x_L}) \\ & \times (-A_L e^{-ik_L x_L} + B_L e^{-k_L x_L} - C_L e^{ik_L x_L} + D_L e^{k_L x_L})^* + \tfrac{1}{4}\rho_L \omega^2 \\ & \times (A_L e^{-ik_L x_L} + B_L e^{-k_L x_L} + C_L e^{ik_L x_L} + D_L e^{k_L x_L}) \\ & \times (A_L e^{-ik_L x_L} + B_L e^{-k_L x_L} + C_L e^{ik_L x_L} + D_L e^{k_L x_L})^*\end{aligned} \tag{A.7}$$

$$\langle e_S \rangle = \tfrac{1}{4} E_S |k_S|^2 \times (G_S e^{-ik_S x_S} - H_S e^{ik_S x_S}) \times (G_S e^{-ik_S x_S} - H_S e^{ik_S x_S})^* + \tfrac{1}{4} \rho_S \omega^2 \times (G_S e^{-ik_S x_S} + H_S e^{ik_S x_S})(G_S e^{-ik_S x_S} + H_S e^{ik_S x_S})^*. \quad \text{(A.8)}$$

Finally, the energy density $\langle e_L \rangle$ and $\langle e_S \rangle$ are spaced-averaged over one wavelength to obtain the analytical expressions for the time- and space-averaged energy density $\langle \underline{e_L} \rangle$ and $\langle \underline{e_S} \rangle$ in the long and the short members, respectively. In all of the analytical solutions the ensemble average response of the system is computed. The ensemble average behavior of the long members is introduced in the analytical solution through a 4% variation assigned to the length of the beams. This is a representative value that has been utilized in the literature for introducing the ensemble average behavior in analytical solutions [35], and has also been utilized for the validation of previous hybrid FEA development [27–29].

References

[1] M.A. Gockel (Ed.), MSC/NASTRAN Handbook for Dynamic Analysis, The MacNeal-Schwendler Corporation, Santa Ana, CA, 1983.

[2] K.J. Bathe, Finite Element Procedures in Engineering Analysis, Prentice-Hall, Englewood Cliffs, NJ, 1982.

[3] K.H. Huebner, E.A. Thornton, The Finite Element Method for Engineers, 2nd Edition, Wiley, New York, 1982.

[4] C.B. Burroughs, R.W. Fischer, F.R. Kern, An introduction to statistical energy analysis, Journal of the Acoustical Society of America 101 (1997) 1779–1789.

[5] C.J. Radcliffe, X.L. Huang, Putting statistics into the statistical energy analysis of automotive vehicles, Journal of Vibration and Acoustics 119 (1997) 629–634.

[6] R.S. Thomas, J. Pan, M.J. Moeller, T.W. Nolan, Implementing and improving statistical energy analysis models using quality technology, Noise Control Engineering Journal 45 (1997) 25–34.

[7] J. Woodhouse, An approach to the theoretical background of statistical energy analysis applied to structural vibration, Journal of the Acoustical Society of America 69 (1991) 1695–1709.

[8] R.H. Lyon, Statistical Energy Analysis of Dynamical Systems: Theory and Applications, The MIT Press, Cambridge, MA, 1975.

[9] O.M. Bouthier, R.J. Bernhard, Simple models of the energetics of transversely vibrating plates, Journal of Sound and Vibration 182 (1995) 149–164.

[10] J.E. Huff, R.J. Bernhard, Prediction of high frequency vibrations in coupled plates using energy finite element, Proceedings of the Inter-Noise '95, Newport Beach, CA, July 1995, pp. 1221–1226.

[11] O.M. Bouthier, Energetics of Vibrating Systems, Ph.D. Dissertation, Mechanical Engineering Department, Purdue University, 1992.

[12] O.M. Bouthier, R.J. Bernhard, Models of space averaged energetics of plates, American Institute of Aeronautics and Astronautics Journal 30 (1992) 138–146.

[13] D.J. Nefske, S.H. Sung, Power flow finite element analysis of dynamic systems: basic theory and applications to beams, Journal of Vibration, Acoustics, Stress and Reliability 111 (1989) 94–106.

[14] N. Vlahopoulos, X. Zhao, T. Allen, An approach for evaluating power transfer coefficients for spot-welded joints in an energy finite element formulation, Journal of Sound and Vibration 220 (1999) 135–154.

[15] N. Vlahopoulos, L.O. Garza-Rios, C. Mollo, Numerical implementation, validation, and marine applications of an energy finite element formulation, Journal of Ship Research 43 (1999) 143–156.

[16] B.R. Mace, The statistical energy analysis of two continuous one-dimensional subsystems, Journal of Sound and Vibration 166 (1993) 429–461.

[17] L. Cremer, M. Heckl, E.E. Ungar, Structure Borne Sound, Springer, New York, 1973.

[18] C.R. Fredo, A SEA-like approach for the derivation of energy flow coefficients with a finite element model, Journal of Sound and Vibration 199 (1997) 645–666.

[19] K. Delange, P. Sas, D. Vandepitte, The use of wave-absorbing elements for the evaluation of transmission characteristics of beam junctions, Journal of Vibration and Acoustics 119 (1997) 293–303.
[20] J.A. Steel, R.J.M. Craik, Statistical energy analysis of structure-borne sound transmission by finite element methods, Journal of Sound and Vibration 178 (1994) 553–561.
[21] C. Simmons, Structure-borne sound transmission through plate junctions and estimates of SEA coupling loss factors using the finite element method, Journal of Sound and Vibration 144 (1991) 215–227.
[22] J.E. Manning, Calculation of statistical energy analysis parameters using finite element and boundary element models, Proceedings of the International Congress in Air- and Structure-Borne Sound and Vibration, Auburn, AL, March, 1990, pp. 771–778.
[23] W. Seeman, Transmission and reflection coefficients for longitudinal waves obtained by a combination of refined rod theory and FEM, Journal of Sound and Vibration 197 (1996) 571–587.
[24] F. Thouverez, M. Viktorovitch, L. Jezequal, A random boundary element formulation for assembled rods and beams in the mid frequency range, in: L. Jezaqual (Ed.), New Advances in Modal Synthesis of Large Structures, Balkema, Rotterdam, 1997, pp. 435–444.
[25] L. Lu, Dynamic substructuring by FEA/SEA, in: S.H. Sung, K.H. Hsu, R.F. Keltie (Eds.), Vehicle Noise, Winter Annual Meeting of the American Society of Mechanical Engineers, Dallas, TX, 1990, pp. 9–12.
[26] R.S. Langley, P. Bremner, A hybrid method for the vibration analysis of complex structural-acoustic systems, Journal of the Acoustical Society of America 105 (1999) 1657–1671.
[27] N. Vlahopoulos, X. Zhao, Basic development of hybrid finite element method for mid-frequency structural vibrations, American Institute of Aeronauties and Astronautics Journal 37 (1999) 1495–1505.
[28] X. Zhao, N. Vlahopoulos, A hybrid finite element formulation for mid-frequency analysis of systems with excitation applied on short members, Journal of Sound and Vibration 237 (2) (2000) 181–202.
[29] N. Vlahopoulos, X. Zhao, An investigation of power flow in the mid-frequency range for systems of co-linear beams based on a hybrid finite element formulation, Journal of Sound and Vibration 242 (3) (2001) 445–473.
[30] J.S. Sun, C. Wang, Z.H. Sun, Power flow between three series coupled oscillators, Journal of Sound and Vibration 189 (1996) 215–229.
[31] B.R. Mace, Power flow between two continuous one-dimensional subsystems: a wave solution, Journal of Sound and Vibration 154 (1992) 289–319.
[32] J.F. Doyle, Wave Propagation in Structures, Springer, New York, 1997.
[33] R.J. Bernhard, J.E. Huff, Structural-acoustic design at high frequency using the energy finite element method, Journal of Vibration and Acoustics 121 (1999) 295–301.
[34] P. Cho, Energy Flow Analysis of Coupled Structures, Ph.D. Dissertation, Mechanical Engineering Department, Purdue University, 1993.
[35] B.R. Mace, Power flow between two coupled beams, Journal of Sound and Vibration 159 (1992) 305–325.
[36] R. Lyon, In-plane contribution to structural noise transmission, Noise Control Engineering Journal (1986) 22–27.